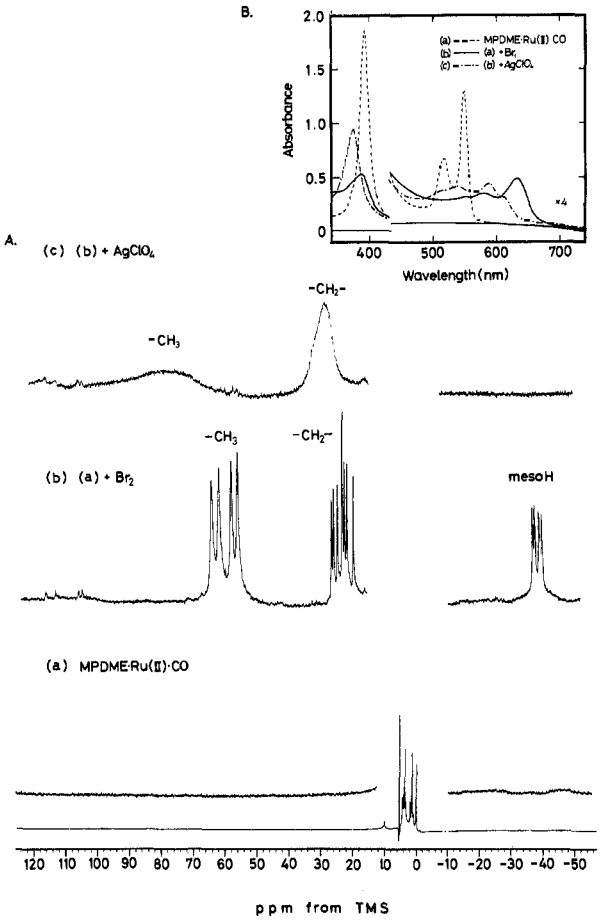

Figure 1. (A) Proton NMR spectra (300 MHz, 22 °C) of the CD_2Cl_2 solution of (MPDME)$Ru^{II}CO$ (ca. 5 mM) in diamagnetic state (a), its one-electron-oxidized π-cation radical [(MPDME)$Ru^{II}CO]^+\cdot Br^-$ (b), and [(MPDME)$Ru^{II}CO]^+\cdot ClO_4^-$ (c). (B) UV–visible spectra of the above compounds.

electron spin density distributions with sign on the prophyrin ring.

Ruthenium(II) porphyrin electrochemically undergoes the ring oxidation to form the π-cation radical for its monocarbonyl complex, while the metal oxidation occurs for the pyridine-ligated complex.[7] These oxidation processes and characterization of the oxidized products have been studied by UV–visible absorption, cyclic voltammetry, and ESR spectroscopic method.[7] We are concerned here with the NMR studies of the Ruthenium(II) porphyrin π-cation radical of which ESR spectrum is not detectable at room temperature. The π-cation radical was formed by the Br_2 oxidation of the CO complex of Ruthenium(II) mesoporphyrin IX dimethyl ester ((MPDME)$Ru^{II}CO$) in methylene chloride solution.[8] This process was followed by the characteristic UV–visible spectrum (Figure 1B) with absorption maxima at 626 and 386 nm, which resembles the spectra of the $^2A_{1u}$ type porphyrin π-cation radicals of other metalloporphyrin complexes.[1] A single ESR signal with $g = 2.003$ and 11-G peak to peak width was obtained at 77 K. The proton NMR spectrum of this radial, [(MPDME)$Ru^{II}CO]^+\cdot Br^-$, is illustrated in Figure 1A, spectrum b.[9,10] The paramagnetically shifted proton peaks are surprisingly sharp and well-resolved, presumably due to very short electron spin relaxation time.[11] This finding appears to correspond to the observation that the ESR spectrum was beyond detection at room temperature due to too much broadening. Br_2 oxidation of the octaethylporphyrin analogue (OEP)$Ru^{II}CO$ also yielded sharp proton resonances at 24 and 30 ppm, readily assignable to the CH_2 protons, and sharp single peak at −35 ppm arising from the meso protons. The unambiguious signal assignments for methyl and meso proton resonances of mesoporphyrin π-cation radical can be made as shown in Figure 1A.

Addition of ClO_4^- ion to the CD_2Cl_2 solution of [(MPDME)$Ru^{II}CO]^+\cdot Br^-$ or [(OEP)$Ru^{II}CO]^+\cdot Br^-$ afforded substantially broadened proton spectrum in the downfield region as exemplified in Figure 1A, spectrum c, and a single-line ESR spectrum with $g = 2.000$ and 12 G peak to peak width at room temperature and with 8-G width at 77 K. The UV–visible spectrum (Figure 1B) was characteristic of an $^2A_{2u}$ type porphyrin π-cation radical, which is formulated as [(MPDME)-$Ru^{II}CO]^+\cdot ClO_4^-$.[1d,e] It is to be noted in Figure 1A, spectrum c, that the meso proton signals were not detected in the upfield or downfield region, in sharp contrast to the spectrum of [(MPDME)$Ru^{II}CO]^+\cdot Br^-$. This was also confirmed by the NMR spectrum of [(OEP)$Ru^{II}CO]^+\cdot ClO_4^-$, which showed a broad CH_2 resonance at 33 ppm and the meso proton peak was beyond detection in the ±2000-ppm spectral region.

We have also examined the proton NMR of the π-cation radicals of other metalloporphyrin complexes. OEPCo^{II} in CD_2Cl_2 solution generates the $^2A_{1u}$ type π-cation radical [(OEP)-$Co^{III}]^{2+}\cdot 2Br^-$ by Br_2 oxidation.[1] This radical did not afford the ESR signal at room temperature, while replacement of $2Br^-$ by $2ClO_4^-$ produced the $^2A_{2u}$ type radical, which was ESR detectable at room temperature.[1] The proton NMR of $[(OEP)Co^{III}]^{2+}\cdot 2Br^-$ exhibited a relatively sharp methylene proton signal at 23 ppm with half-line width of 900 Hz and a broad meso proton peak at −81 ppm.

An isotropic shifts of −45 ppm (upfield) at 275 K for the meso proton of [(OEP)$Ru^{II}CO]^+\cdot Br^-$ and −91 ppm for [(OEP)-$Co^{III}]^{2+}\cdot 2Br^-$ are translated into spin densities of 0.027 and 0.054, respectively, at the meso carbon π-orbital, which are more than 10 times as much as the corresponding value (0.0012) calculated by SCF–CI MO method for the metal-free porphyrin π-cation radical ($^2A_{1u}$).[1c] An absolute value of a meso proton ESR coupling constant, 1.48 G, measured[1c] for [(OEP)$Mg^{II}]^+\cdot ClO_4^-$ corresponds to a π-spin density of 0.066, comparable to the present NMR results. Since an a_{1u} π-cation orbital has a node at the meso

(7) Brown, G. M.; Hopf, F. R.; Furguson, J. A.; Meyer, T. J.; Whitten, D. G. *J. Am. Chem. Soc.* **1973**, *95*, 5939–5942. Rillema, D. P.; Agle, J. K.; Barringer, L. F., Jr.; Meyer, T. J. *Ibid.* **1981**, *103*, 56–62. Kadish, K. M.; Chang, D. *Inorg. Chem.* **1982**, *21*, 3614–3618. Kadish, K. M.; Leggett, D. J.; Chang, D. *Ibid.* **1982**, *21*, 3618–3622.

(8) The equimolar amount of Br_2 was added to the CD_2Cl_2 solution of (MPDME)$Ru^{II}CO$ to yield a one-electron-oxidized species, which was readily reduced to the starting material by KI. With the excess Br_2, further oxidized species was formed and was not reduced by KI.

(9) Proton NMR spectra were obtained at 300 MHz on a Nicolet NT-300 spectrometer equipped with a 1280 computer system. There was no noticable concentration dependence on the line width of the proton spectrum of this radical. The visible spectrum persisted after the NMR spectrum was recorded.

(10) The hyperfine shift pattern for the species in Figure 1A, spectrum b, and for [(OEP)$Ru^{II}CO]^+\cdot Br^-$ appears to resemble that for the ferric high-spin porphyrin complexes. This may allow one to expect that Ru^{III} high-spin state could be responsible for the NMR hyperfine shifts. This possibility is, however, ruled out on a basis of the observations that the ESR spectrum is characteristic of the doublet free radical, the visible spectrum matches that expected for a porphyrin π-cation radical and that the magnetic susceptibility measurement by the Evans method shows the $S = {}^1/_2$ state ($\mu_{eff} = \sim 1.8\mu_B$). Collman et al., reported the NMR spectrum of a (OEP)Ru^{II} dimer ($S = 1$), which has a CH_2 signal near that shown in Figure 1A, spectrum b, (Collman, J. P.; Barnes, C. E.; Collins, T. J.; Brothers, P. J.; Gallucci, J.; Ibers, J. A. *J. Am. Chem. Soc.* **1981**, *103*, 7030–7032.). However, the meso H of this dimer is located at 10 ppm in the downfield region, which contrasts to the upfield shift in Figure 1A, spectrum. The possibility of Ru^{III} low-spin state is also ruled out by the NMR measurement of the low-spin complex (OEP)$Ru^{III}(py)_2$, which afforded single methyl resonance at 23 ppm (Shiro and Morishima, unpublished results). The finding that the one-electron-oxidized species of (MPDME)$Ru^{II}CO$ and (OEP)$Ru^{II}CO$ is readily reduced by a mild reducing reagent, KI, may also support that one electron is extracted from the porphyrin ring rather than the metal.

(11) The reason for short electron spin relaxation time is not clear at the present stage. Quite a normal value of $g = 2.003$ for these radicals may allow us to expect that a spin–orbit coupling at metal atom may not be responsible for enhanced electron spin relaxation. Coupling of metal orbitals and π-levels or counteranion and π-radical could cause the short electron spin relaxation.[1d,e] Degenerate or nearly degenerate radicals may also exhibit enhanced relaxation caused by electron exchange between two states. The unusual non-Curie law behavior of the meso proton resonance of the OEP$Ru^{II}CO$ π-cation radical could be due to this cause.

(12) La Mar, G. N.; de Ropp, J. S.; Latos-Grazynski, L.; Balch, A. L.; Johnson, R. B.; Smith, K. M.; Parish, D. W.; Cheng, R.-J. *J. Am. Chem. Soc.* **1983**, *105*, 782–787.

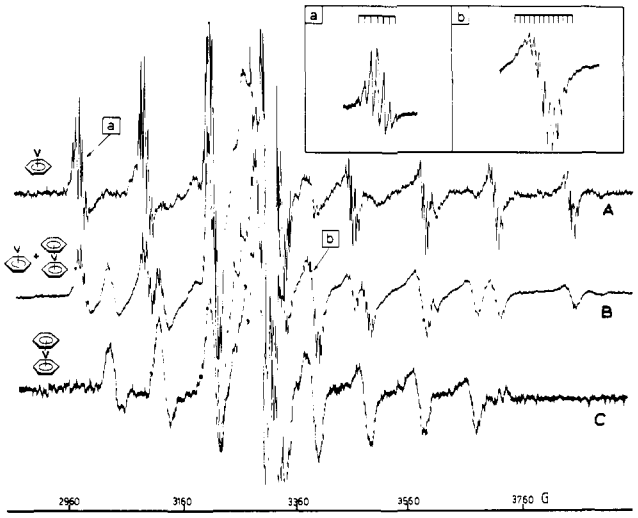

Figure 1. Electron paramagnetic resonance spectra for the products of the cocondensation of V atoms with C_6H_6/Ar matrices at 12 K (A) C_6H_6/Ar $\simeq$ 1/250, (B) C_6H_6/Ar $\simeq$ 1/50, and (C) the same as (B) but after annealing to 40 K. Inserts a and b show selected vanadium hyperfine components of $(\eta^6\text{-}C_6H_6)V$ in a and $(\eta^6\text{-}C_6H_6)_2V$ in b.

When V atoms are cocondensed with high dilution C_6H_6/Ar $\simeq$ 1/50–1/250 matrices at 12 K, V/Ar $\simeq$ $1/10^4$, the optical spectra, besides displaying the characteristic resonance lines of isolated V atoms,[4] shows a prominant new absorption around 550 nm. On 12–40-K annealing, the V atomic lines gradually decay to zero with the concomitant production of the 320- and 450-nm absorptions of the $(\eta^6\text{-}C_6H_6)_2V$ complex. The growth–decay behavior of the new 550-nm absorption under these conditions is typical of a reactive intermediate as described in the scheme below:

$$V + C_6H_6 \rightarrow (C_6H_6)V;\ 550\ nm$$

$$(C_6H_6)V + C_6H_6 \rightarrow (C_6H_6)_2V;\ 320,\ 450\ nm$$

The EPR spectra of these dilute V/C_6H_6/Ar matrices are most informative. Typical traces for C_6H_6/Ar $\simeq$ 1/250 and 1/50 are depicted in Figure 1A,B and the outcome of 40-K annealing of the 1/50 matrix is shown in Figure 1C. Expanded traces of selected vanadium hyperfine lines showing proton superhyperfine components are also illustrated as inserts a and b in Figure 1.

The features of immediate interest in these EPR spectra are (i) the observation of the eight vanadium hyperfine lines (rigid limit) of $(\eta^6\text{-}C_6H_6)_2V$ in 1/50 but *not* in 1/250 C_6H_6/Ar matrices, (ii) the observation of eight *new* vanadium hyperfine lines (also of the rigid limit type) co-existing with those of $(\eta^6\text{-}C_6H_6)_2V$ in 1/50 C_6H_6/Ar matrices but standing *alone* in 1/250 matrices, (iii) the formation of $(\eta^6\text{-}C_6H_6)_2V$ at the expense of the new (benzene)vanadium complex on annealing the 1/50 matrices at 40 K, and (iv) the observation of resolved proton superhyperfine splitting for $(\eta^6\text{-}C_6H_6)_2V$ as well as the new (benzene)vanadium complex where the small proton thirteen-line coupling $\langle a\rangle(13, {}^1H) \simeq 4.26$ G and seven-line coupling $\langle a\rangle(6, {}^1H) \simeq 5.35$ G are diagnostic of the interaction of the unpaired electron with *twelve* and *six* equivalent protons respectively. The complex signal around 3300 G is due to hydrocarbon radicals resulting from some extraneous cracking of benzene on the hot vanadium filament.

These data unequivocally establish the existence of $(\eta^6\text{-}C_6H_6)_2V$ and $(\eta^6\text{-}C_6H_6)V$ in concentrated and dilute C_6H_6/Ar matrices, respectively, where molecular tumbling perpendicular to the C_6 axis has been frozen out, leading to anisotropic vanadium hyperfine splitting; yet the twelve and six protons respectively appear to be spatially and magnetically equivalent resulting in essentially isotropic proton superhyperfine splitting. The resolution of the proton superhyperfine splitting in $(\eta^6\text{-}C_6H_6)_2V$ and $(\eta^6\text{-}C_6H_6)V$ is found to decrease as the free benzene concentration in the matrix increases showing no fine structure at all in solid C_6H_6, where only $(\eta^6\text{-}C_6H_6)_2V$ is detectable. This effect can be ascribed to guest–host interactions that restrict the rotational averaging of the superhyperfine tensors of the coordinated benzene ring(s) with respect to the C_6 axis of the complexes, resulting in magnetic inequivalence of the protons and line broadening. The observation of larger $a_\perp(^{51}V)$ and $a(^1H)$ coupling constants for $(\eta^6\text{-}C_6H_6)V$ indicates that the unpaired electron density is greater on both the vanadium atom and the benzene ring protons in $(\eta^6\text{-}C_6H_6)V$ as compared with $(\eta^6\text{-}C_6H_6)_2V$. The actual observation of resolved proton superhyperfine splitting in solid Ar, implies the existence of rather spacious multiple substitutional matrix trapping sites for both $(\eta^6\text{-}C_6H_6)V$ and $(\eta^6\text{-}C_6H_6)_2V$ and the facile rotation of these molecules about their C_6 axes in this matrix support.

Computer simulation of the EPR spectra for $(\eta^6\text{-}C_6H_6)V$ and $(\eta^6\text{-}C_6H_6)_2V$ in the rigid support limit has been carried out, and preliminary static effective spin Hamiltonian tensor components are found in Table I.

These data show quite clearly that the ground-state electronic configuration, structure, and bonding properties of $(\eta^6\text{-}C_6H_6)_2V$ are not greatly perturbed on removing one of the benzene rings to form $(\eta^6\text{-}C_6H_6)V$. This proposal receives support from the

Table I

	$(\eta^6\text{-}C_6H_6)V$	$(\eta^6\text{-}C_6H_6)_2V$
$g_\parallel$	≅1.989	≅1.986
$g_\perp$	1.945	1.981
$a_\parallel(^{51}V)$	≅9.35 G	≅10.2 G
$a_\perp(^{51}V)$	117.30 G	93.57 G
$a_\parallel(^1H)$	≅5.2 G	≅4.3
$a_\perp(^1H)$	≅5.4 G	≅4.2

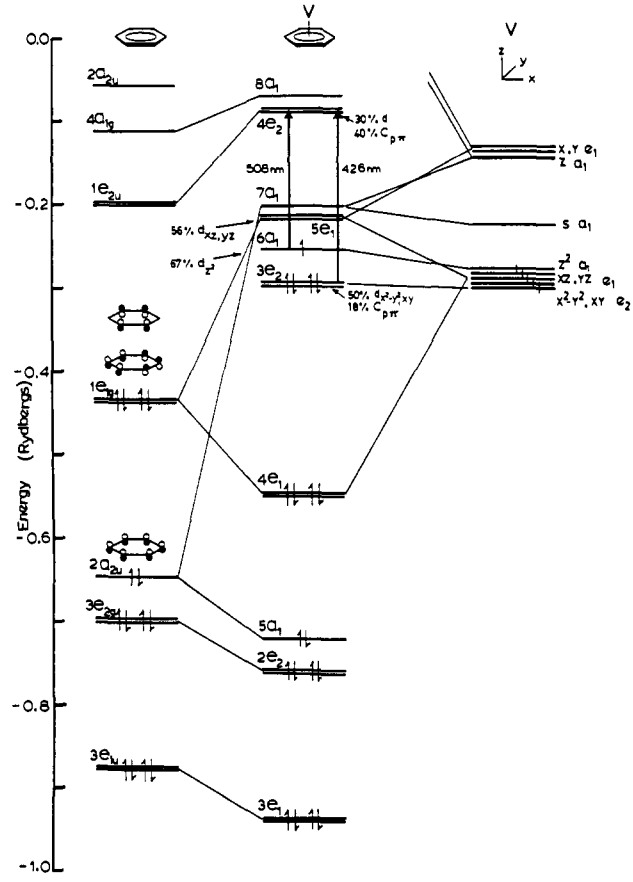

Figure 2. Ground-state, spin-restricted, SCF-Xα-SW MO energy level scheme for C_{6v}, $(\eta^6\text{-}C_6H_6)V$. The energies of the two electronic excitations indicated refer to those calculated by Slater transition-state procedures. The distance between the vanadium atom and the C_6-ring center of gravity is 1.66 Å (ref 1) in this calculation.

(4) Ozin, G. A.; Klotzbücher, W.; Mitchell, S. A. *Inorg. Chem.* **1977**, *16*, 3063.

results of our SCF-Xα-SW MO calculation for C_{6v}, $(\eta^6\text{-}C_6H_6)V$, summarized in Figure 2. In this description one finds (i) the degenerate $1e_{1g}$ π-level of benzene, stabilized mainly by interaction with valence $d_{xz,yz}$ orbitals on V and with negligible contributions in the $5a_1$ level from V s and p valence orbitals, giving rise formally to two strong V-C_6H_6 bonding levels housing four electrons $5a_1^2 4e_1^4$, (ii) two V valence orbitals d_{z^2} and d_{xy} remaining essentially metal localized with a small bonding contribution from the $d_{x^2-y^2}$ symmetry set and containing five electrons $3e_2^4 6a_1^1$, and (iii) three empty low-lying V-C_6H_6 antibonding orbitals $5e_1(d_{xz,yz})$ and $7a_1(s, d_{z^2})$. Overall, this scheme results in a $^2A_1$ ground electronic state for $(\eta^6\text{-}C_6H_6)V$ with an orbital picture and bonding scheme essentially the same as that of the $^2A_{1g}$ ground-state parent $(\eta^6\text{-}C_6H_6)_2V$ sandwich. Finally, the Xα transition-state calculations favor a $3e_2^4 6a_1^1 \rightarrow 3e_2^4 6a_1^0 4e_2^1$ mainly metal-to-ligand charge-transfer assignment for the 550-nm absorption of $(\eta^6\text{-}C_6H_6)V$ as indicated in Figure 2.

Acknowledgment. We acknowledge the Natural Sciences and Engineering Research Council of Canada for financial assistance.

Registry No. $(C_6H_6)V$, 61332-91-0; V, 7440-62-2; C_6H_6, 71-43-2.

Direct Heterolysis of a Very Weak Carbon-Carbon Bond to a Carbocation and Carbanion

Edward M. Arnett,* E. B. Troughton, Andrew T. McPhail,* and Kent E. Molter

Paul M. Gross Chemical Laboratory, Duke University Durham, North Carolina 27706

Received June 24, 1983

Carbocations and carbanions are the two most important types of ionic species in organic chemistry. Most discussions of organic reaction mechanisms have revolved around the effects of structural change on the thermodynamic or kinetic stability of these species or of transition states that are presumed to be close to them in energy. The simplest of polar reactions to form carbon–carbon bonds should be those involving the direct coordination of carbocations with carbanions since wide variation of the structure of both species should be possible and no allowance need be made for the involvement of leaving groups or catalysts. Correspondingly, the direct heterolysis of carbon–carbon bonds to form the two types of carbon ions should offer similar advantage. Although most carbocations and carbanions are too unstable to coexist in the same solvent, we have shown in a recent communication[1] that, with sufficient stabilization of both species, the coordination reaction can be slowed to the point where kinetic study is convenient or even to the point where no observable reaction takes place over a period of 6 mo at room temperature. An important goal that is suggested by such a study has been to find a series of compounds for which the coordination and heterolysis reactions are so well balanced that the equilibrium between covalent and ionic species can be studied and with a measureable rate for either the coordination or heterolysis reaction. This implies the design of a series of compounds with such weak carbon-to-carbon bonds that they may be broken to form ions simply by dissolving them. Such a compound is represented by I.

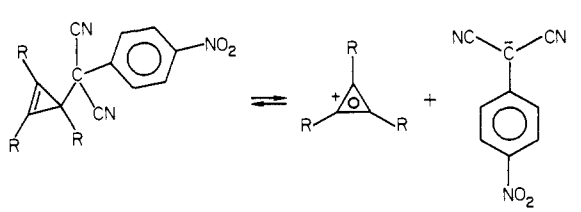

I, R = CH_3
II, R = phenyl

(1) Arnett, E. M.; Troughton, E. B. *Tetrahedron Lett.*, in press.

Compound I was prepared by the reaction of trimethylcyclopropenium tetrafluoroborate with potassium (*p*-nitrophenyl)malononitrile in acetone solution. After the precipitated potassium tetrafluoroborate was removed by filtration and evaporating the solvents, the colorless product was taken up in a benzene–hexane mixture, filtered, and then cooled to produce crystals. A single-crystal X-ray analysis[2] defined the structure and solid-state conformation to be as presented in Figure 1. The crystal structure was solved by direct methods.[3] Full-matrix least-squares adjustment of atomic parameters[4] (anisotropic C, N, O; isotropic H) converged to $R^5 = 0.064$ over 1559 statistically significant reflections.[6] The results of this study reveal an unusually long bond length between the malononitrile and cyclopropane ring carbon atoms [C(1′)–C(1) 1.588 (4) Å >> C(1)–C(4) 1.485 (5) Å] as well as a lesser, but still significant, elongation in the adjacent bond to the phenyl ring [C(1′)–C(1″) 1.552 (4) Å].

Although crystals of I and their solution in diethyl ether are colorless at room temperature, the orange color of the carbanion appears at once if the crystals are dissolved in acetone or any more polar solvent. In chloroform solution at room temperature the ^1H NMR spectrum shows a broad signal at δ 1.88 for the carbocation, which on cooling to −50 °C resolves into two signals at δ 2.07 (6 H) and 1.29 (3 H) corresponding to the covalent product. These frequencies correspond almost exactly with those reported by Closs and Harrison[7] for trimethylcyclopropenium azide in CH_2Cl_2. Thus, the X-ray crystal structure provides unequivocal evidence for the existence of a covalent compound that on dissolution in polar solvents dissociates into a trimethylcyclopropenium cation and a (*p*-nitrophenyl)malononitrile carbanion. A quantitative investigation of the equilibrium between covalent and ionic species for this system is presently under way and will be reported later.[10]

The following results have been obtained for the equilibrium properties of the closely related triphenylcyclopropenium (*p*-nitrophenyl)malononitrile (II) system for which the ^{13}C NMR, infrared spectra, and elemental analysis confirm, by close analogy to compound I, the formation of a covalent crystalline material. Equilibrium constants for the covalent–ionic process were determined in six different solvents by monitoring the absorbance of the (*p*-nitrophenyl)malononitrile anion (λ_{max} = 475–490 nm, ε = 30 000). The Debye–Hückel limiting law, which is valid for compound II in acetonitrile, was used to correct[8] equilibrium constants for ionic strength effects resulting from heterolysis. In accordance with expectation, an excellent linear relation between the free energy of heterolysis, $\Delta G_{het}°$, and $1/D$ was found, as predicted by the Born equation (Figure 2).[10]

Equilibrium constants were also determined at several temperatures to yield the enthalpy of reaction both when approached by coordination of the ions ($\Delta H_{coord}° = -5.4 \pm 0.3$ kcal mol^{-1}) or as approached independently by heterolysis of the covalent compound ($\Delta H_{het}° = +5.5 \pm 0.5$ kcal mol^{-1}). As an independent check, the enthalpy of reaction of the ions was determined calorimetrically by thermometric titration of a solution of the cation into an excess of potassium (*p*-nitrophenyl)malononitrile[9] ($\Delta H_{coord}°$

(2) Crystal data: $C_{15}H_{13}N_3O_2$, M,267.30, triclinic, a = 7.684 (3) Å, b = 15.115 (6) Å, c = 7.248 (3) Å, α = 77.88 (1)°, β = 117.85 (1)°, γ = 106.73 (1)°, U = 710.0 Å^3, Z = 2, d_{calcd} = 1.250 g cm^{-3}, space group $P\bar{1}(C_i^1)$.

(3) Main, P.; Lessinger, L.; Woolfson, M. M.; Germain, G.; Declerq, J.-P. "MULTAN76, a System of Computer Programmes for the Automatic Solution of Crystal Structures"; Universities of York and Louvain, 1976.

(4) See paragraph at end of paper regarding supplementary material.

(5) $R = \Sigma||F_o| - |F_c||/\Sigma|F_o|$.

(6) Intensity data were recorded on an Enraf-Nonius CAD-3 automated diffractometer (Ni-filtered Cu Kα radiation, λ = 1.5418 Å; θ–2θ scans, θ_{max} = 67°) by use of procedures detailed elsewhere, see: Miller, R. W.; McPhail, A. T. *J. Chem. Soc., Perkin Trans. 2* 1979, 1527.

(7) Closs, G. L.; Harrison, A. M. *J. Org. Chem.* **1972**, *37*, 1051.

(8) This correction was less than 25% of K for all solvents, corresponding to a 0.15 kcal mol^{-1} change in $\Delta G_{het}°$.

0002-7863/83/1505-6172$01.50/0